CONCEPTUAL DESIGN AND SIZING OF A SOLAR POWERED QUAD-ROTOR FIXED WING HYBRID UAV FOR EXPLORATION OVER MARS

Kalgutkar, A.¹, Gupta, P.¹, Priyadarshi, P.² & Pant, R. S.¹

¹Indian Institute of Technology Bombay, Mumbai, Maharashtra, 400076, India ²Vikram Sarabhai Space Centre, Trivandrum, Kerala, 695022, India

Abstract

This paper presents a comprehensive conceptual design for a solar-powered hybrid unmanned aerial vehicle (UAV) specifically tailored for Mars exploration. The proposed configuration combines quadcopter vertical takeoff and landing capabilities with fixed wings for horizontal propulsion, supported by solar energy harvesting. The study utilizes a design methodology derived from a literature review of a similar UAV configuration on Earth, adapting it to the unique challenges and environmental conditions of Mars. Additionally, simulation parameters are modified to accurately represent Martian conditions, including the incorporation of an illumination model and solar cell methodologies. The design process involves the generation and evaluation of multiple design points based on desired mass, payload capacity, and endurance, offering a range of feasible options for Martian UAV missions. The selected configuration has four motors in a quadcopter configuration for Vertical Take-Off and Landing (VTOL) along with fixed wings and a single motor for horizontal propulsion. Energy is harvested using body-mounted solar cells over the duration of a Martian day to enable high endurance flight. The literature review is conducted to obtain a design methodology (albeit without solar power) for a similar configuration of vehicle for earth. This methodology is implemented and the code is validated. Design points are generated and evaluated for feasibility. Several vehicle configurations are presented based on the desired mass, endurance and assumed irradiance threshold. Simulations are performed for different mission profiles to study battery State of Charge versus time. A sensitivity analysis is conducted for estimated parameters (Figure of Merit and C_L/C_D limit) to account for a degree of uncertainty.

Keywords: Conceptual Design, Solar Powered, Hybrid UAV, Mars Exploration

1. Introduction

The human ambition to explore other planets may be greatly augmented with the use of Unmanned Aerial Vehicles (UAVs) enabling large areas to be studied significantly faster as compared to a ground-based rover. With the successful flight of Ingenuity as part of the Mars 2020 mission, the feasibility of sustained powered flight on Mars has been demonstrated and more comprehensive vehicles may be envisaged. Any design under consideration must have sufficient endurance to carry out surveys while carrying a payload of scientific instruments. It is important to determine an appropriate configuration for the UAV and obtain estimates through a preliminary design and sizing study before progressing to detailed analysis.

Mars presents a challenging environment for aviation on account of the extremely low atmospheric density (0.015 kg m⁻³). Surface temperatures reach below -70 °C at night necessitating heaters and consequently an energy reserve to survive the inhospitable thermal environment. The solar irradiance received by Mars (586.2 W/m²) is severely diminished in comparison to the Earth (1361.0 W/m²) on account of the increased distance to the sun. Solar panels are assumed to be the sole source of energy for this study and the reduced irradiance contributes to the challenges of flight on Mars. Further, the climate on Mars is known for severe dust storms which may severely restrict if not completely stop solar energy from reaching the surface.

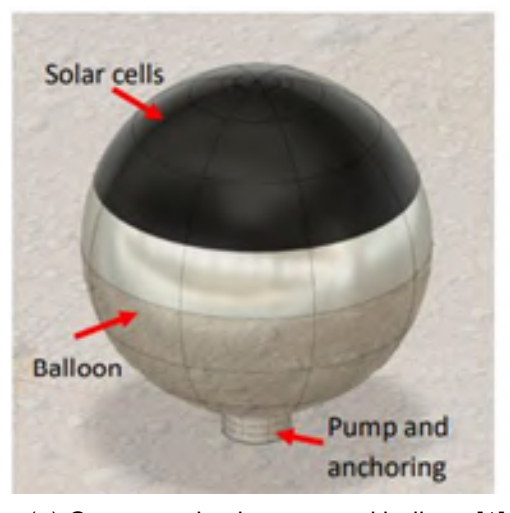
Additional considerations must be made for packaging the vehicle into a 2.65 m diameter Viking-derivative aeroshell for entry, descent and landing. The low atmospheric density necessitates a large wingspan greater than 5 m requiring a stowage mechanism. The exact configuration of the stowage system is not considered in the preliminary sizing analysis but a mass budget must be allocated.

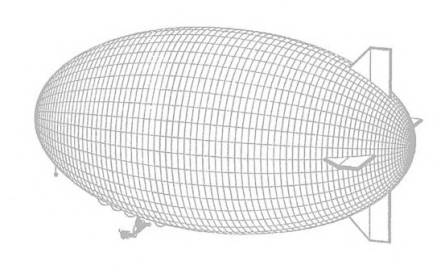
2. Literature Review

A detailed survey of literature of the various hybrid vehicles that have been proposed for the exploration of Mars during the past 35 - 40 years was carried out and roughly 60 research papers/articles and reports were thoroughly studied. Based on the operational capabilities of the UAVs, the vehicles have been classified into four categories on the basis of their configuration:

2.1 Lighter-than-Air Systems:

As the name suggests, these vehicles use the concept of buoyancy to generate lift force and can be deployed in the Martian atmosphere. These are lightweight as compared to fixed wing aircraft. The main advantage of using an LTA system is that it can be airborne for a longer endurance as it produces its lift from Buoyancy. We can store it in the launch vehicle in a short space and can be deployed once it enters the Martian atmosphere. Some research has been done on this configuration and provided in [1–7]. A conceptual image of Solar Powered LTA balloon is shown in Fig. 1a [1].





- (a) Conceptual solar powered balloon [1]
- (b) Conceptual solar powered balloon [7]

Figure 1 – Proposed lighter-than-air concepts

2.2 Fixed Wing UAV:

This is the simplest UAV which can be designed but the aircraft must be modular in nature to store it in the shell or capsule of the launch vehicle, thus the aircraft must possess a folding mechanism or have inflatable wings for its use. An image of *MiniSniffer-III* [8] is shown in Fig. 2a which was designed to operate in the Martian atmosphere but tested in the Earth atmosphere, and detailed research were carried out for fixed wing configuration and given in [8–35].

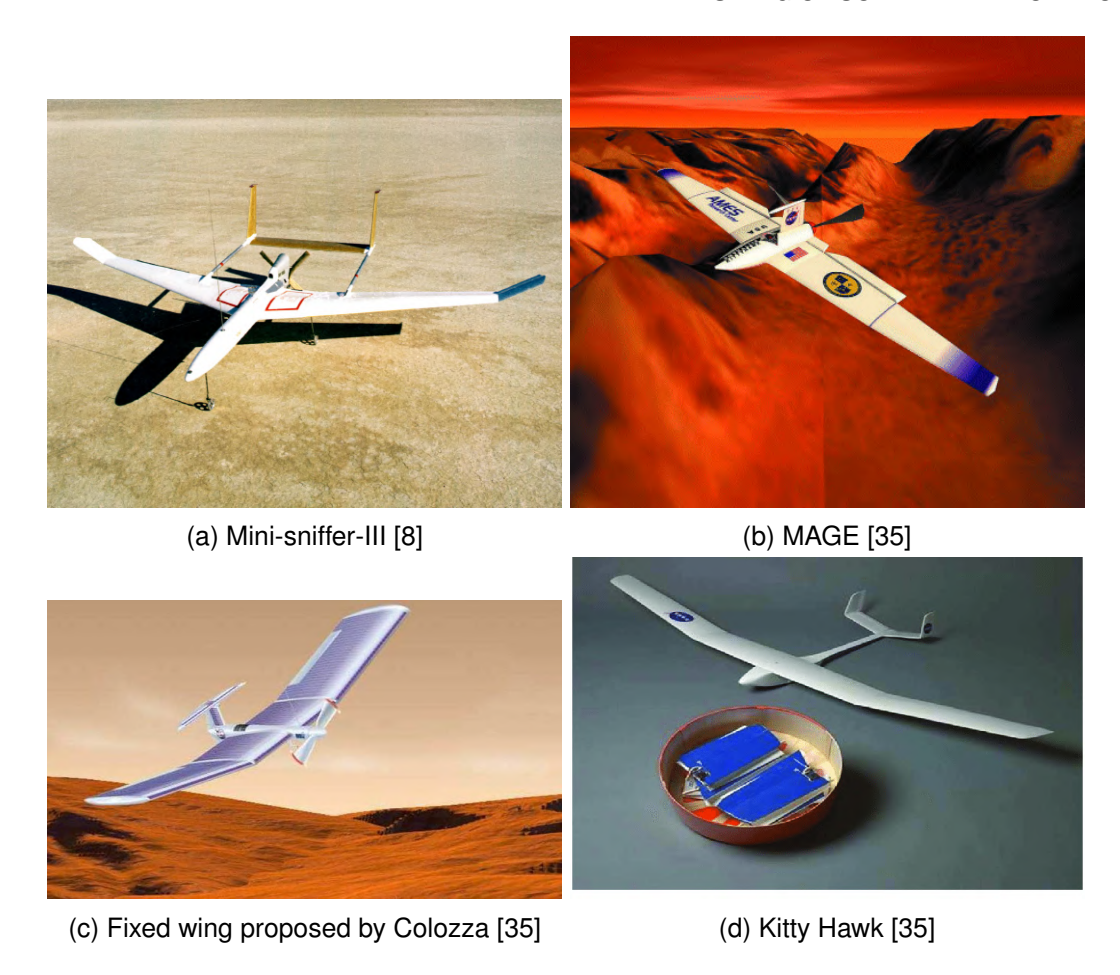


Figure 2 – Proposed fixed wing UAV concepts

2.3 Rotary wing Aircraft:

Rotary wing aircraft i.e., Ingenuity as shown in Fig. 3a consumes more power than any other configuration and relies on onboard storage systems thereby having limited operation time. Detailed research has been carried out on this configuration and given in [36–41].

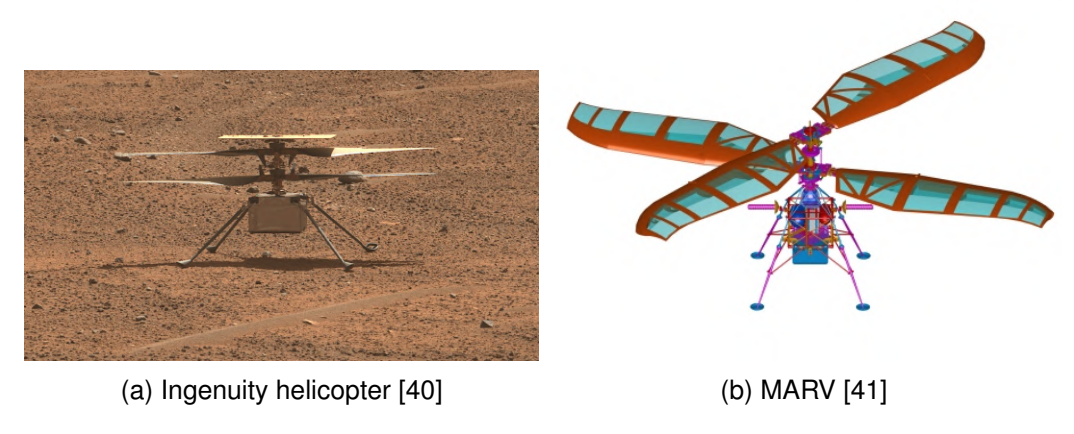


Figure 3 - Proposed rotary UAV concepts

2.4 Hybrid Vehicles:

These types of vehicles can be the combination of any two configurations i.e., Lighter-than-Air and Fixed wing aircraft or combination of Fixed wing and Rotary wing aircrafts as shown in Fig. 4a [42] depending upon the mission requirements. This can be a promising configuration for a UAV on Mars. An artistic CAD model is shown in Fig. 4b. Detailed research on hybrid Martian vehicles has been carried out and provided in [42–48].

The existing research papers and reports have been carefully analyzed and promising vehicle configurations have been identified. These configurations are summarized in Table 1.

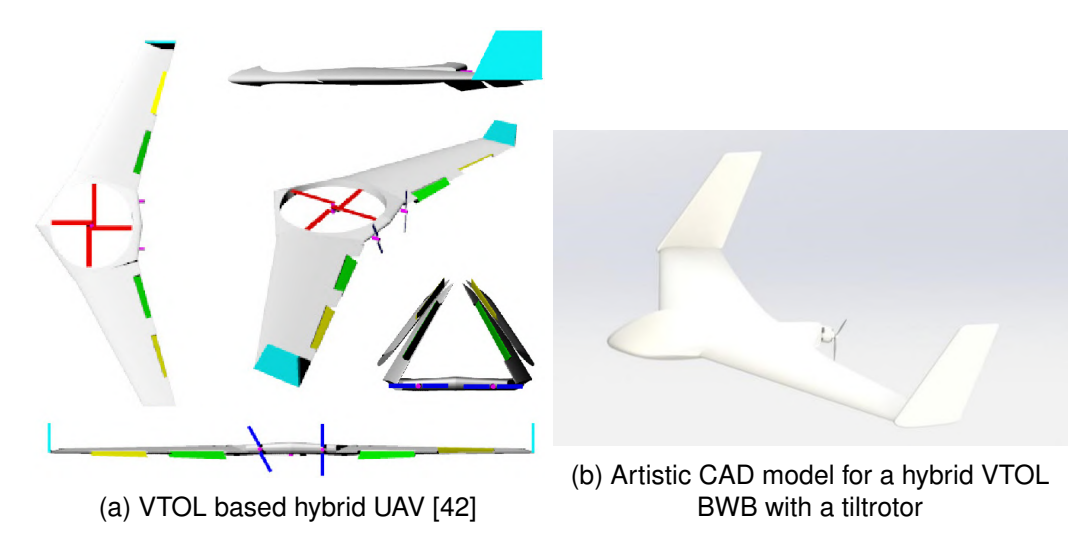


Figure 4 – Proposed hybrid UAV concepts

Table 1 – Promising configurations for Martian a UAV

Type of Vehicle	Vehicle Configuration	
Rotary Wing UAV	Solar Powered Carbon-dioxide balloon	
Fixed Wing	Twin-boom Configuration	
Hybrid UAV	Quadcopter and fixed wing combination	

3. Configuration Selection

Through an extensive literature survey, we have successfully identified several configurations that hold great promise in addressing the research objectives. These configurations have been subjected to a comprehensive comparative analysis, the results of which are presented in Table 2.

Table 2 - Comparison of UAV configurations

Configuration	Advantages	Disadvantages	
Determination (114)/	Simple control scheme, no transition	High energy consumption	
Rotary Wing UAV	between flight modes required		
	Already proven on Mars	Limited endurance and payload	
	Simple control scheme, no transition	Lack of smooth runway on Mars	
Fixed-Wing Vehicle	between flight modes required	for take-off and landing	
	High cruise velocity	Wings are not compact	
Lighter-Than-Air	In general, have the greatest endurance	Very large in volume	
Lighter-man-All	out of the given configurations	Are susceptible to unfavourable	
		weather conditions	
Hybrid UAV	Higher endurance compared to purely rotary vehicles	High number of motors	
	Can operate from rough terrain unlike	VTOL motors are dead weight	
	FW vehicles	during FW flight	

Based on the meticulous comparative analysis and in-depth study conducted, a hybrid UAV configuration has been determined as the most suitable choice. The comprehensive evaluation of various factors and performance indicators has led to the conclusion that this configuration possesses the desired attributes and capabilities necessary to fulfill the objectives of the research. An illustration of a similar vehicle is provided in Figure 5.

The proposed design combines the ability of a quadcopter to operate on uneven terrain with the greater endurance and reduced energy consumption of a fixed-wing aircraft. The control scheme for quadcopters is well understood and there are no major attitude changes required while transition from VTOL to fixed-wing flight. Additionally, a large wing area allows for greater solar power generation in flight which serves to increase the endurance.

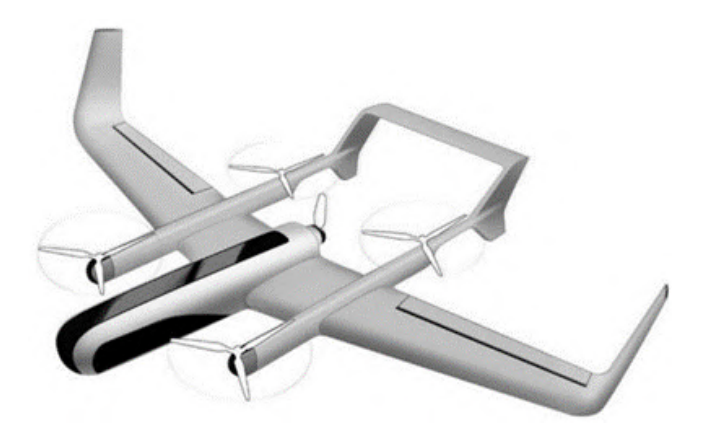


Figure 5 – Quad-rotor fixed wing hybrid UAV [49]

4. Mission Overview

The launch vehicles employed in Mars exploration generally comprise a Lander, which is deployed from a Mother Ship and approaches the Martian surface at an atmospheric entry speed of approximately 7.3 km/s. However, if a UAV is launched from the Lander during the atmospheric entry phase, it must undergo deceleration to attain subsonic velocities. Consequently, during this deceleration phase, the Lander will have advanced considerably ahead of the UAV. To facilitate examination of the landing vicinity, the Lander incorporates an onboard gimbal-mounted camera. This camera enables the Lander to survey the surrounding area and determine the optimal heading for exploration on Mars. The envisioned UAV for this mission will be solar-powered, constructed using lightweight and non-corrosive materials. It will also be equipped with a small surveillance camera and an RF link to communicate with satellites. To enable versatile flight capabilities, the UAV will feature adjustable propellers that facilitate both forward flight and vertical flight for hovering.

4.1 Mission Profile

The proposed vehicle conducts a vertical take-off, using the four motors mounted in a quadcopter configuration. As it ascends to the cruising altitude, the fifth motor which provides propulsion in the fixed-wing mode is activated and the horizontal velocity reaches the cruise speed. This is sufficient to generate lift from the wing airfoil and the VTOL motors can be deactivated. In cruise mode, the vehicle flies at the cruise velocity using the single motor drawing energy from the battery. This accounts for the majority of the flight duration. Once the mission is completed and a suitable landing site identified, the VTOL motors are activated and the horizontal velocity is allowed to drop below the stall speed. The vertical landing is carried out in quadcopter mode. A reserve of endurance in the hovering mode is maintained to account for any difficulties experienced while identifying a landing zone. This mission profile is illustrated in Figure 6.

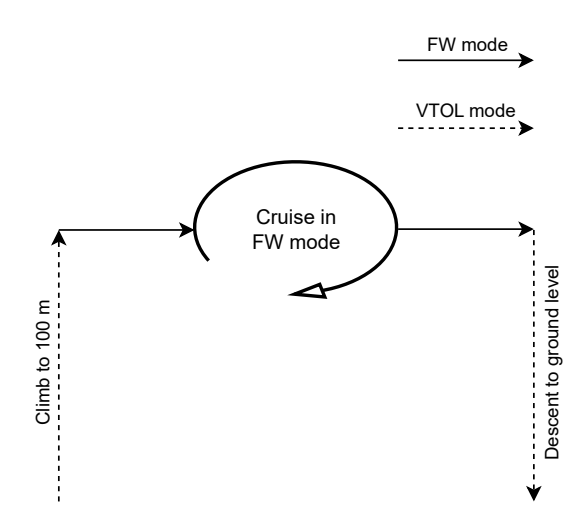


Figure 6 – Mission profile of the proposed UAV

4.2 Mission Requirements

After conducting an extensive review of the available literature on unmanned aerial vehicles (UAVs) and their associated mission requirements, a rigorous and systematic analysis was undertaken to identify the key parameters essential for attaining optimal performance and gaining a competitive advantage in our vehicle. The critical requirements identified through this process have been consolidated and presented in Table 3, encapsulating the essential aspects that must be considered for our proposed vehicle.

Table 3 – Design constraints and requirements for Martian VTOL UAV

Parameter	Value
Total Weight	≤ 100 kg
Operating Altitude	100 m
Payload Weight	≥ 5 kg
Endurance	\geq 60 seconds
Modularity	Fit within a 2.65 m diameter Viking-derivative aeroshell shape
Atmosphere	Martian Reference Atmosphere

5. Methodology

The methodology employed for the development of a hybrid quadcopter fixed-wing UAV is derived from the work presented by Maxim Tyan et al. [49] (Fig. 7). A preliminary estimate of the vehicle mass is obtained from initial guess values by analyzing individual subsystems including the VTOL propulsion, fixed-wing propulsion, and the battery. The vehicle is then resized iteratively until convergence is achieved. This approach encompasses various modules designed to ensure the selection of feasible design points based on constraints analysis. The methodology proposed by Tyan et al. relies on an external charging source whereas the present study focuses on an independent vehicle, resulting in the need to include a solar energy module. An irradiance model proposed by VanderMey [50] has been adapted to represent the variation in solar irradiance over the duration of a sol. Mass estimates of solar cells and the maximum power point tracking (MPPT) system are obtained utilizing the methodology presented by Noth [51]. From the irradiance and solar cell models, the energy generated by the UAV is obtained which is compared to the energy consumed in flight activities. This ensures that the generated design points maintain a net energy balance over a given sol, enabling daily flights.

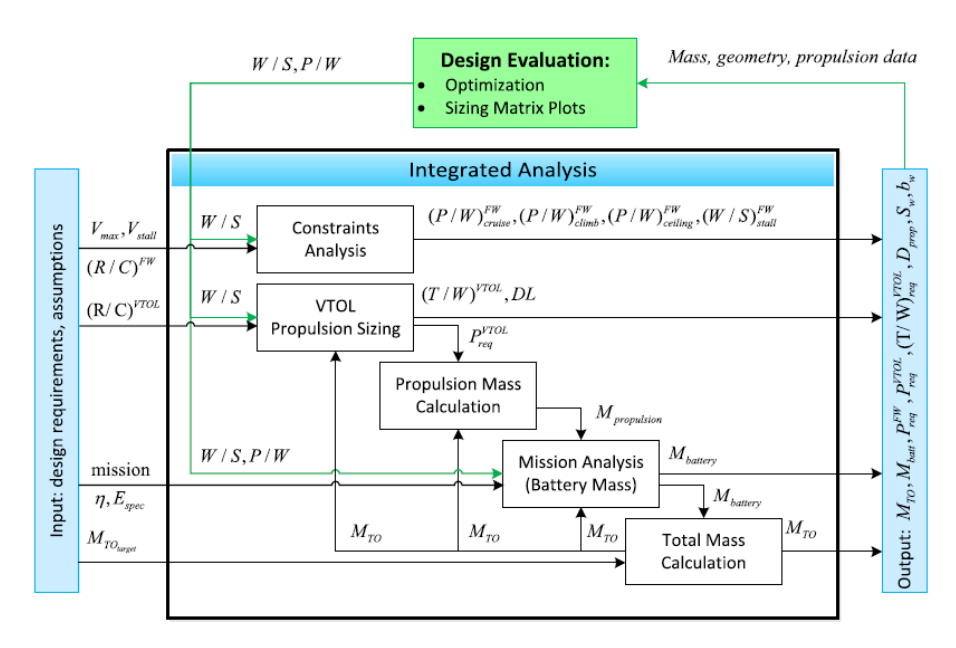


Figure 7 – Design methodology given by Tyan et al. [49]

5.1 Design Point Generation and Iteration Loop

The initial step of the methodology is the generation of potential design points through a systematic process involving parameter iteration. This process encompasses various vehicle parameters such as the Aspect Ratio (AR), wing loading, and mission-specific factors including cruise velocity, endurance, and maximum solar irradiation for a given day. The upper and lower bounds for the iteration parameters used are provided in Table 4. Additional input parameters used are enumerated in Table 5.

Table 4 – Parameters used for design point generation

Parameter	Lower Bound	Upper Bound
Wing Loading	16 N/m ²	49 N/m ²
Cruise Velocity	68 m/s	120 m/s
Aspect Ratio	5	20
Cruise Endurance	60 seconds	Maximum achievable

Table 5 – Parameters that are constant or assumed constant

Parameter	Value	Unit	Description
g	3.72	[m/s ²]	Gravity of Mars
ρ	0.015	[kg/m ³]	Air density of Mars
μ	1.4×10^{-5}	[Pa.s]	Air viscosity of Mars
I _{max}	586.2	[W/m ²]	Maximum irradiance
k _{att}	0.7	-	Solar attenuation coefficient
е	0.8	-	Oswald's efficiency factor
C _{D0}	0.1	-	Zero-lift coefficient of drag
C _{Lmax}	0.8	-	Maximum value of coefficient of lift
(C _L /C _D) _{max}	4	-	Maximum ratio of coefficient of lift to coefficient of drag
η_{prop}	0.75	-	FW propeller efficiency
FM	0.55	-	Figure of Merit
MF _{struct}	0.40	-	Mass fraction of structure
MF _{avionics}	0.05	-	Mass fraction of avionics
MF _{subsys}	0.15	-	Mass fraction of miscellaneous subsystems
MF _{stowage}	0.10	-	Mass fraction of stowage system
E _{spec}	180*3600	[J/kg]	Energy density of battery
η_{batt}	0.95	-	Battery efficiency
$\eta_{ ext{charge}}$	0.95	-	Battery charging efficiency
$\eta_{ m electric}$	0.87	-	Electric motor efficiency
f _{usable}	0.75	-	Battery usable fraction (reserve capacity)
k _{sc}	0.32	[kg/m ²]	Mass density of solar cells
k _{en}	0.26	[kg/m ²]	Mass density of encapsulation
$\eta_{ extsf{sc}}$	0.169	-	Efficiency of solar cells
η_{cbr}	0.90	-	Efficiency of curved panels
k _{mppt}	0.00042	[kg/W]	Mass to power ratio of MPPT
η_{mppt}	0.97	-	MPPT efficiency
q _{fill}	8.0	-	Fraction of wing area with solar cells

The take-off mass of each potential design point is calculated iteratively. This iteration continues until either convergence is achieved or the value diverges, resulting in the rejection of the design point. Within each iteration of the loop, distinct modules are employed to address specific aspects of the design process. An aerodynamics module is utilized to determine the necessary thrust during flight. Additionally, fixed-wing and VTOL propulsion modules appropriately size the motors and associated components such as propellers and electronic speed controllers (ESCs). A solar power module estimate the mass and peak energy production of the solar cells and maximum power point tracking (MPPT) system. Furthermore, an overall mass module generates the take-off mass as the final output of the iteration,

By incorporating these modules into the iterative loop, the design process for the hybrid quadcopter fixed-wing UAV is systematically guided, enabling the exploration of various design points and the optimization of critical parameters.

5.2 Aerodynamics Module

The aim of the aerodynamics module is to specify constraints based on the aerodynamics of the vehicle. Two constraints are imposed in this module. the first specifying that the cruise velocity should exceed the stall velocity by at least 20% to provide a sufficient safety margin during flight. The second constraint mandates that the ratio of the lift coefficient to the drag coefficient (C_L/C_D) must not surpass 4, aiming to address potential RPM issues with the motor. Design points failing to meet these criteria are considered invalid and are consequently rejected.

Parameters such as the stall velocity and the optimal velocities for climb and endurance, are computed based on the wing loading and aspect ratio values provided during the design point generation

step. The optimal velocity values are used for the cruise and climb phases if these satisfy the stall margin constraint. The cruise velocity value specified by the iteration loop is used instead if the constraint is not met.

The thrust-to-weight ratios during cruise and climb are required to determine the power consumed during the respective phases. These values are obtained using the following equations:

$$(W/S)_{Stall}^{FW} = \frac{1}{2}\rho V_{stall}^2 C_{Lmax} \tag{1}$$

$$(T/W)_{Cruise}^{FW} = qC_{D0}\frac{1}{(W/S)} + k\frac{1}{q}(W/S)$$
 (2)

$$(T/W)_{Climb}^{FW} = \frac{R/C}{V_{RoC}} + qC_{D0}\frac{1}{(W/S)} + k\frac{1}{q}(W/S)$$
(3)

Where q and k are given by:

$$q = \frac{1}{2}\rho V^2, k = \frac{1}{\pi eAR}$$

These equations enable the precise evaluation of thrust requirements relative to the weight of the hybrid quadcopter fixed-wing UAV during different flight phases. By incorporating these calculations into the overall methodology, a comprehensive understanding of the aerodynamic characteristics and propulsion needs of the vehicle is obtained, leading to informed decision making during the design process.

It is assumed that key factors including the maximum coefficient of lift (C_{Lmax}), zero-lift drag coefficient (C_{D0}), and Oswald efficiency factor (e) remain constant across all design points.

5.3 Fixed-Wing Propulsion Module

The fixed-wing propulsion system consists of a single motor and propellor. In each iteration, the required thrust output is obtained from the thrust-to-weight ratio provided by the aerodynamics module along with the mass estimate from the previous iteration. The maximum power consumption is calculated based on the generated thrust using equation 4.

$$P = \frac{TV_{cruise}}{\eta_{prop}} \tag{4}$$

5.4 VTOL Propulsion Module

The Vertical Take-Off and Landing (VTOL) propulsion module is similar to the fixed-wing propulsion module. It consists of four rotors in a quadcopter configuration with two blades per motor. The maximum thrust-to-weight ratio of 1.5 is chosen to provide a sufficient reserve margin in the event of gusts. The power consumption in VTOL mode is calculated using the desired rate-of-climb using equation 5.

$$P_{req}^{VTOL} = \frac{Tv_i}{FM} \tag{5}$$

Where v_i is the induced velocity in axial climb and v_h is the induced velocity during hover.

$$v_i = -(V_{RoC}^{VTOL}/2) + \sqrt{(V_{RoC}^{VTOL}/2)^2 + v_h^2}$$
 (6)

$$v_h = \sqrt{\frac{T}{2\rho S_p}} \tag{7}$$

Empirical relations derived for terrestrial conditions cannot be used to determine the Figure of Merit (FM) of the VTOL propellers on account of the vastly different conditions of the Martian atmosphere. Experimental performance figures from Shrestha et al. [52] for a rotor in an evacuation chamber at the appropriate atmospheric density and Reynolds number range are used to estimate an appropriate

FM. A FM \geq 0.55 is attainable at Reynolds numbers greater than 20,000 with respect to the rotor tip speed. Furthermore, an increase in the FM is observed with an increasing value of Re. Using figures from Fujita et al. [53], a rotor blade of radius 1.8 meters, aspect ratio of 6 with a blade tip Mach number of 0.75 would result in a Reynolds number of approximately 50,000. This ensures that a value of 0.55 for the FM can be safely assumed. An additional sensitivity study to capture the variation in the vehicle mass for changes in the FM is conducted in Section 6.3

5.5 Solar Power Module

The wing-mounted solar cells generate power during flight and recharge the battery on the ground between missions. The solar cells are assumed to cover a fixed proportion of the overall wing area. The mass per unit area of the cells along with the encapsulation hardware is known, giving the total mass. The mass of the Maximum Power Point Tracker (MPPT) is determined using an empirical relation, with the peak power generated by the cells as the input. This value is found using the solar cell area and the illumination model as discussed below. The illumination model used assumes the solar irradiance to vary sinusoidally across the duration of the day, with the value of the solar irradiance being zero at dawn, the maximum irradiance achieved at midday and dropping to zero by sunset. This allows for the irradiance to be calculated as a function of the time elapsed since sunrise. The irradiance model is represented by equation 8.

$$I(t) = I_{max} \sin(\pi \frac{t}{t_{day}}) \tag{8}$$

Where t is the elapsed time since sunrise and t_{day} is the total sunlight duration (from sunrise to sunset).

The curve presented in Figure 8 provides an explanation for the irradiance model used. A Martian day (or sol) lasts for 24 hours, and 39 minutes with sunlight lasting for 12 hours. The sinusoidal irradiance model assumes a peak value of 586.2 W/m² before atmospheric attenuation. Due to seasonal variation and atmospheric phenomena such as dust storms, the actual intensity received is expected to be significantly less than the ideal value. To account for this, the vehicle is designed with a constant irradiance (eg. 100 or 200 W/m²), At greater intensities of solar radiation, the endurance and number of flights per sol increases significantly.

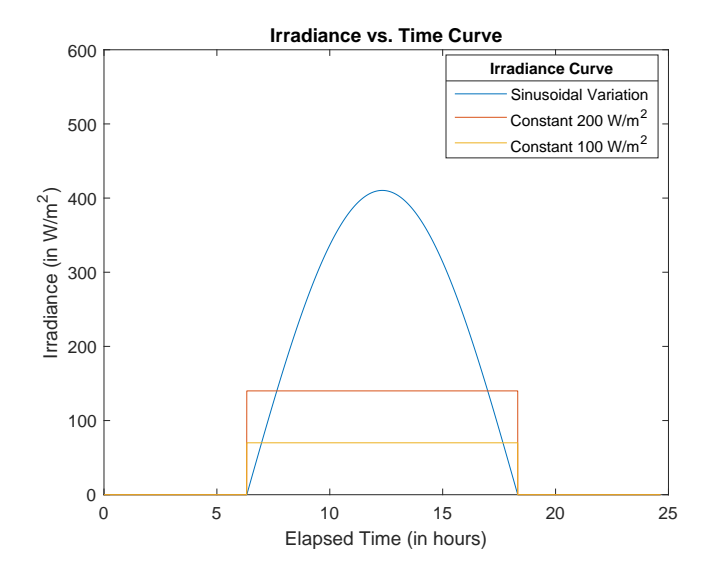


Figure 8 – Martian irradiance model

5.6 Energy Module

The sizing and mass estimation for the battery is performed in this module. The battery capacity is calculated to provide sufficient energy for one flight in addition to a energy reserve expressed as a fraction of the overall capacity. The energy consumption per flight is obtained as the sum of the

energy requirements during each phase of flight (vertical take-off, transition to FW flight, cruise in FW mode and landing) minus the simultaneous energy generation from the solar cells.

5.7 Mass Module

The mass of the remaining elements of the vehicle must be estimated to obtain the mass estimate which is used as the input for the next iteration of the loop.

Using empirical relations provided by Tyan et al., the masses of the motors, propellers and Electronic Speed Controllers (ESCs) can be obtained from the maximum power consumption of both the VTOL and FW motors. The following relations are used to calculate the masses of the motors, propellers and ESCs. Note that all propellers are assumed to be fabricated from composite materials.

$$\frac{W_{mot}}{P_{max}} = F_1 P_{max}^{E_1} U_{max}^{E_2} \tag{9}$$

$$M_{prop} = 6.514 \times 10^{-3} K_{material} K_{prop} n_{props} n_{blades}^{0.391} \left(\frac{D_{prop} P_{prop,max}}{1000}\right)^{0.782}$$

$$(10)$$

$$M_{ESC} = F_{ESC} P_{max}^{E_3} \tag{11}$$

The airframe, avionics components and other subsystems (unaccounted for in this study) are assumed to have a fixed mass fraction. Conversely, the sum of the masses of the solar cells FW and VTOL propulsion and battery accounts for the remainder of the mass fraction of the vehicle.

The wingspan of the UAVs studied are on the order of 10-15 m which is significantly more than can be accommodated in a 2.65m diameter Viking-style aeroshell. Greater wingspan enables increased endurance for a desired mass limit. A mechanism to stow the wings in an aeroshell is required. The exact design of such a mechanism is beyond the scope of the present study. To account for this omission, a mass budget of 10% is included. Since the exact mass and mass fraction of these components is known, the total take-off mass of the vehicle can be obtained at the end of an iteration using equation 12. This value is used as the input for the next iteration loop and so on until convergence is obtained.

$$M_{TO} = \frac{M_{propulsion}^{VTOL} + M_{propulsion}^{FW} + M_{payload} + M_{solar}}{1 - (MF_{batt} + MF_{struct} + MF_{subsyst} + MF_{avion} + MF_{stowage})}$$
(12)

6. Results

A design point is feasible if the take-off mass converges within a certain number of iterations. Further, it is evaluated based on various criteria for it to be deemed viable. For example, the total mass of the vehicle should not exceed a certain threshold value, the selected cruise velocity must be at least 20% greater than the stall velocity and the energy generated over the course of a day by the solar cells should be greater than the energy consumed in flight. If all conditions are met, the design point can be taken forward for a detailed design study.

6.1 Comparative Analysis

Comparative analysis plots of the wingspan versus vehicle mass as displayed in Fig. 9 were generated for different input values of the threshold irradiance parameter. The graphs contain only the optimal vehicles for a target endurance and not every feasible design point. Multiple vehicles are displayed for certain endurance values where alternate configurations may offer reduced mass at the cost of increased wingspan or vice versa. Note that endurance refers to the duration of fixed wing cruise in a flight.

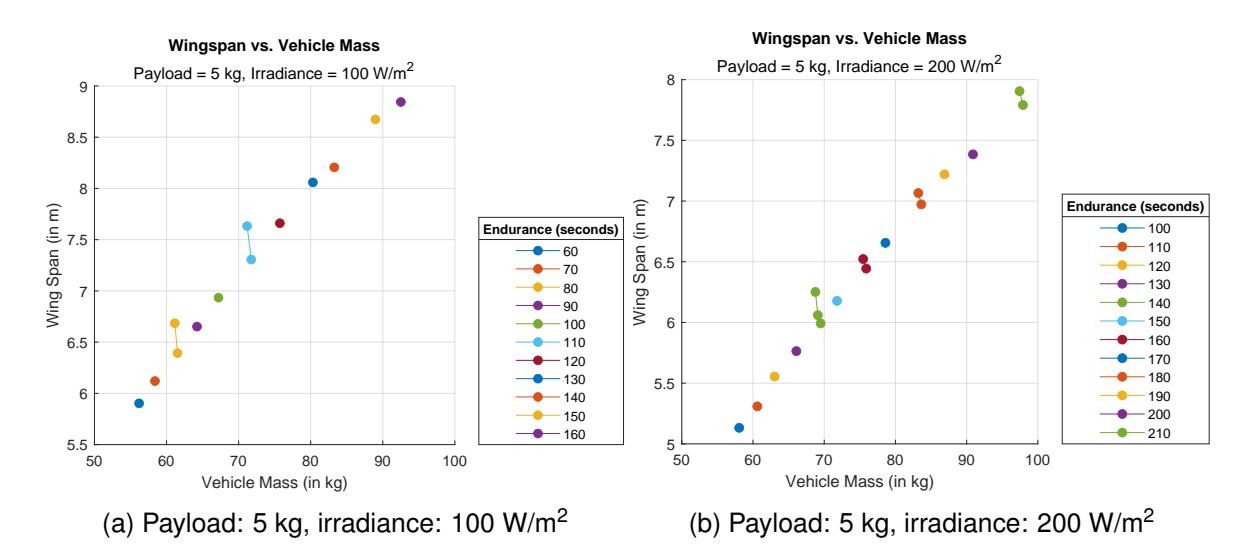


Figure 9 – Sample comparative analysis curves generated using preliminary methodology

Two design points for a threshold irradiance of 100 W/m² are provided in Tables 6 and 7 to illustrate the trade off between mass and endurance. Subsequent analysis is carried out only for the high endurance configuration.

Table 6 - Sample specifications for high endurance UAV

Parameter	Value
Vehicle Mass	92.50 kg
Payload	5 kg
Irradiance Assumed (Constant Value)	100 W/m ²
Endurance (in FW cruise)	160 sec
Reserve hovering capacity	30 sec
Wingspan	8.84 m
Wing Loading	22 N/m ²
Aspect Ratio	5
Cruise Speed	79 m/s
Rate of Climb (FW and VTOL)	2 m/s
Propeller Diameter (FW)	1.07 m
Maximum Power per Motor (FW)	9.99 kW
Propeller Diameter (VTOL)	3.70 m
Maximum Power per Motor (VTOL)	4.46 kW

6.2 Battery Consumption Study

The variation in the battery state of charge with the time of day is studied for various mission profiles including flying at dawn, flying at noon, flying at dusk and multiple flights per sol. In each scenario, the vehicle first climbs to the cruise altitude in VTOL mode before flying in FW mode until the energy required for descent would exceed the battery capacity excluding 25% held in reserve. The energy calculations include 30 seconds of hovering flight which may be used during the transition to FW flight or during powered descent. The vehicle configuration selected (described in Table 6) is designed with a threshold irradiance of 100 W/m² to guarantee a minimum cruise duration. For this analysis, a sinusoidal irradiance model (Equation 8) with a peak intensity of 586.2 W/m² before atmospheric attenuation is selected to obtain the endurance under realistic illumination conditions.

6.2.1 Single Flight Analysis

The battery State of Charge across the duration of a sol is graphed in Fig. 10 for multiple simulated mission profiles. In the first scenario (Fig. 10a), the vehicle begins flight immediately at dawn while the

Table 7 – Sample specifications for low mass UAV

Parameter	Value
Vehicle Mass	56.20 kg
Payload	5 kg
Irradiance Assumed (Constant Value)	100 W/m ²
Endurance (in FW cruise)	60 sec
Reserve hovering capacity	30 sec
Wingspan	5.90 m
Wing Loading	30 N/m ²
Aspect Ratio	5
Cruise Speed	93 m/s
Rate of Climb (FW and VTOL)	2 m/s
Propeller Diameter (FW)	0.98 m
Maximum Power per Motor (FW)	7.12 kW
Propeller Diameter (VTOL)	2.88 m
Maximum Power per Motor (VTOL)	2.71 kW

irradiance is less than the threshold value. The endurance marginally decreases though recharging is completed before noon, potentially enabling multiple flights per sol. In the second scenario (Fig. 10b), the vehicle takes off only after the irradiance has exceeded the threshold value, enabling the target endurance to be achieved. Similar to the previous case, recharging is completed by noon enabling further missions in the sol. For the third scenario (Fig. 10c), the flight is centred about noon. The endurance increases to 173 seconds due to the increased irradiance provided by the realistic sinusoidal curve compared to the constant threshold assumption. In the fourth scenario (Fig. 10d), the vehicle is flies just before sunset where the irradiance has dropped below the threshold value. Recharging cannot be completed before sunset. Though heat loss and heating requirements during the Martian night are not modelled in this study, the importance of reserve battery capacity is highlighted here.

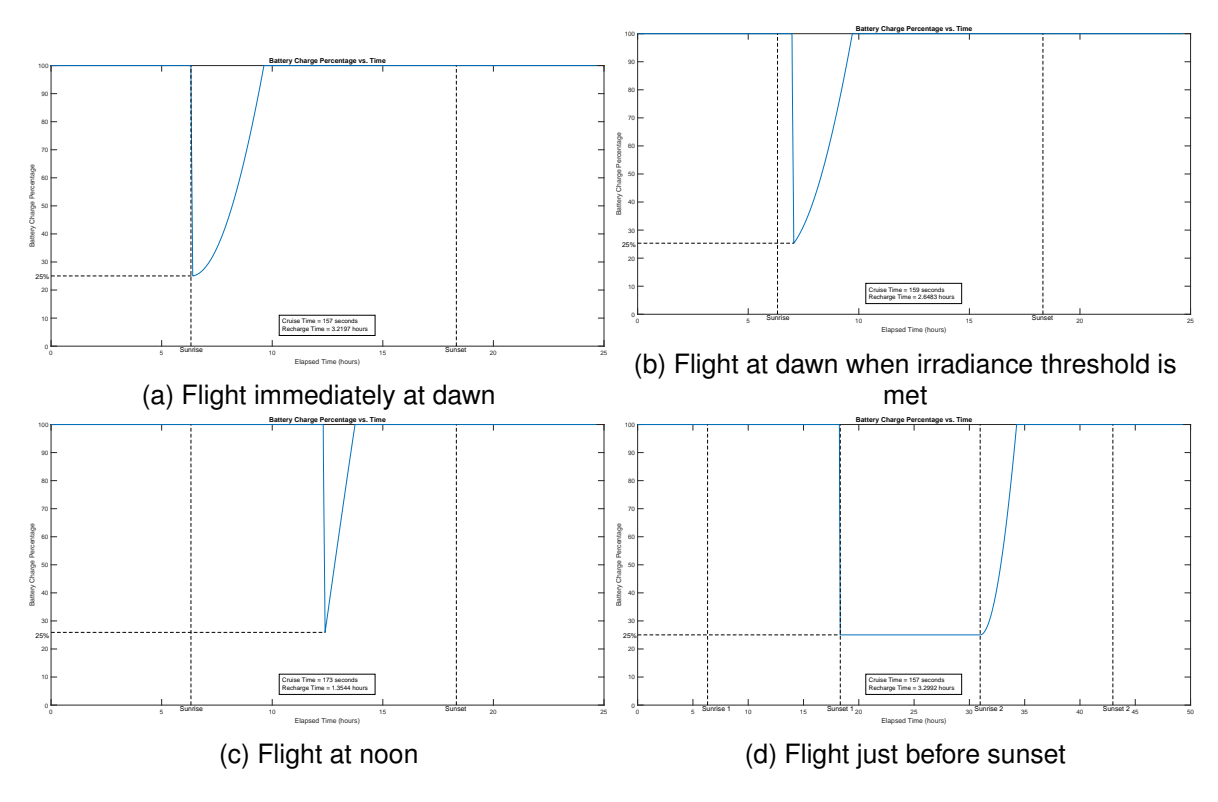


Figure 10 – Battery state of charge for different mission profiles

6.2.2 Battery Consumption Study: Multiple Flight Analysis

From the results obtained in Section 6.2.1 it is evident that multiple flights may be conducted per sol. This possibility was studied using the same vehicle configuration (Table 6) and irradiance model as the single flight analysis.

The vehicle first takes off after sunrise once the irradiance threshold of 100 W/m₂ is crossed. Missions are conducted as per the same guidelines as the previous section except the vehicle is permitted to take off again once the battery is fully recharged. This process continues until insufficient daylight remains to recharge the battery should another flight occur. Using this methodology it was determined that up to five flights are possible over the course of a sol. The cruise endurance and subsequent recharging times are provided in Table 8 and the variation of the battery State of Charge with time is displayed in Fig. 11. A total cruise duration of 843 seconds per sol was obtained through this approach. This level of endurance is impractical to achieve in a single flight due to the high power requirement for flight on Mars and consequently the large battery mass fraction required.

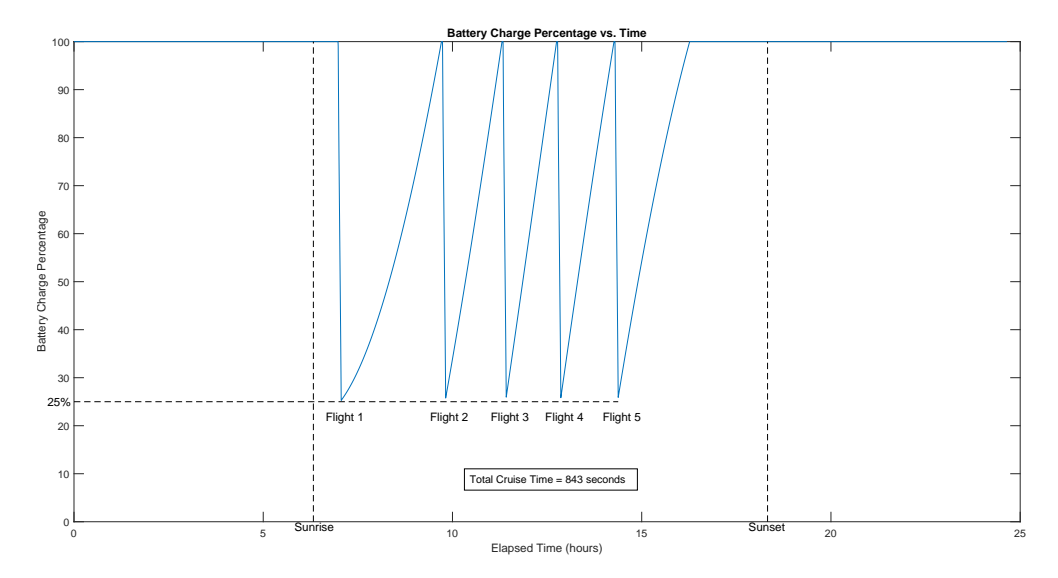


Figure 11 – Battery state of charge for multiple flights

Table 8 – Summary of multiple flights over a sol

Flight Number	Cruise Endurance	Recharging time
1	159 sec	2.65 hours
2	169 sec	1.49 hours
3	172 sec	1.33 hours
4	173 sec	1.40 hours
5	170 sec	1.89 hours

6.3 Sensitivity Analysis

A sensitivity analysis study is conducted for two input parameters, namely the Figure of Merit (FM) for the vertical propulsion propellers and the maximum limit for the ratio of the coefficient of lift to the coefficient of drag (C_L/C_D). Estimates for these parameters are used in the above sections which introduces a degree of uncertainty. Performing a sensitivity analysis allows for the effects of variations to be known before proceeding further to a more comprehensive design study.

6.3.1 Figure of Merit

The Figure of Merit assumed for all vehicle configurations is 0.55 from the experimental results obtained by Shrestha et al. [52]. Increasing the rotor Reynolds number results in an improvement in the value of the FM and for Re \geq 50,000 the FM approaches a maximum of 0.62. The effect of varying the Figure of Merit on the vehicle mass is plotted in Fig. 12 for a constant cruise endurance of 160

seconds. For this analysis the value of FM was treated as an additional iteration parameter and the feasible design point with the lowest mass is displayed. Note that the maximum mass constraint of 100 kg was relaxed to showcase the effects of reduced FM.

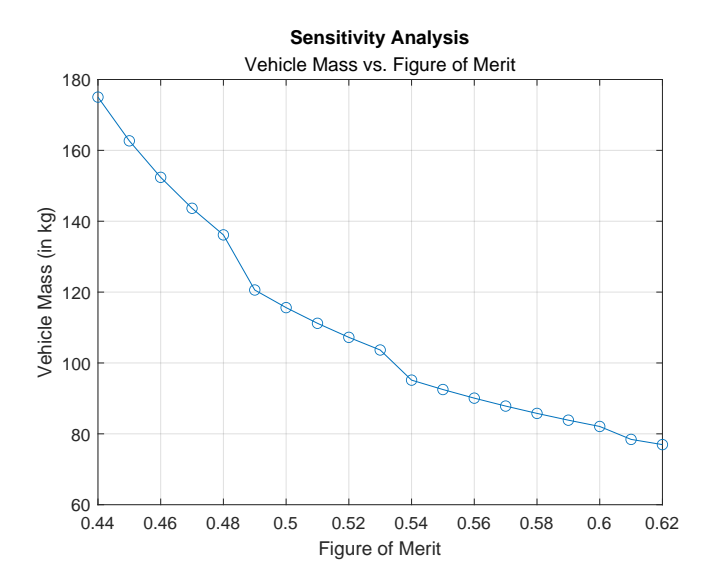


Figure 12 – Sensitivity analysis for figure of merit

6.3.2 C_I/C_D

A restriction on the ratio of the coefficient of lift to the coefficient of drag is imposed due to dynamics and controls considerations. This limit is set to 4 for the present preliminary design study, although a more detailed analysis may increase or decrease this value. The constraint imposed on C_L/C_D results in a limitation on the maximum permissible coefficient of lift and hence the minimum flight velocity (separate from the stall velocity). Alternate configurations are not analysed in this section since this limitation is not inherent to the design of the vehicle in terms of the parameters examined in this study. The effects of varying the maximum permissible C_L/C_D on the cruise endurance are showcased in Table 9 using same vehicle configuration outlined in Table 6 in all cases. Note that the single flight at noon case is analysed as shown in Figure 10c.

Table 9 − Sensitivity analysis for C_L/C_D limit

C _L /C _D Limit	Cruise Endurance	Required Cruise Velocity	V _{Cruise} /V _{Stall}
3	105 sec	94.97 m/s	1.57
4	173 sec	78.96 m/s	1.30
5	272 sec	65.26 m/s	1.08
6	316 sec	60.55 m/s (Flying at Stall)	1

The constraint on C_L/C_D may be converted to a quadratic inequality (Equation 14) by expressing C_D in terms of C_L (Equation 13). Should the quadratic equation have a negative discriminant (Equation 15), the inequality is always satisfied and the vehicle may fly up to the stall velocity without encountering any dynamics and controls limitations. For the configuration under consideration, this results in a minimum required limit of 5.6 to allow for flight at stall.

$$C_D = C_{D0} + kC_L^2 (13)$$

$$kC_L^2 - \frac{C_L}{\mathsf{Limit}} + C_{D0} \ge 0 \tag{14}$$

$$limit > \frac{1}{\sqrt{4kC_{D0}}} \tag{15}$$

7. Conclusions

A preliminary design study for a solar powered quadrotor fixed wing hybrid UAV has been performed which indicates the feasibility of the configuration. Multiple feasible designs are proposed for a 5 kg payload capacity for a takeoff mass up to 100 kg. A cruise endurance of 170 seconds may be achieved under favourable illumination conditions along with 50 seconds of ascent, 30 seconds of hovering and 50 seconds of descent for a total flight duration of 300 seconds. The vehicle performance was investigated for different irradiance conditions across various times of the sol. It was determined that conducting multiple flights in a sol enables a total cruise endurance in excess of 800 seconds over up to five flights without any additional mass penalty. A sensitivity analysis study is included to account for any uncertainties while estimating input parameters. Further scope includes refining the aerodynamic parameter estimation (C_L , C_{Lmax} , C_{D0}) and the airframe mass estimation. A stability analysis and empennage sizing may be performed in a subsequent investigation. Further, an energy consumption model for the transition phase between vertical and horizontal flight would improve the battery size estimation.

8. Contact Author Email Address

The corresponding author, Pranav Gupta can be contacted at the email address below: pranavgupta0711@gmail.com

9. Copyright Statement

The authors confirm that they, and/or their company or organization, hold copyright on all of the original material included in this paper. The authors also confirm that they have obtained permission, from the copyright holder of any third party material included in this paper, to publish it as part of their paper. The authors confirm that they give permission, or have obtained permission from the copyright holder of this paper, for the publication and distribution of this paper as part of the ICAS proceedings or as individual off-prints from the proceedings.

References

- [1] Wade Hisiro, Matthew Julian, Elisa Pantoja, Arpan Sinha, George Wilkes, and Mool C Gupta. Photovoltaic balloon for autonomous energy generation on mars (mega-pb). 2018.
- [2] Robert M Zubrin, Terry Gamber, and Steve Price. *The Mars Aerial Platform Mission: A Global Reconnaissance of the Red Planet Using Super-Pressure Balloons*. AIAA, 1993.
- [3] A Vargas, J Evrard, P Mauroy, A Vargas, J Evrard, and P Mauroy. Mars 96 aerostat-an overview of technology developments and testing. In *International Balloon Technology Conference*, page 1449, 1997.
- [4] Viktor V Kerzhanovich, James A Cutts, and Jeffery L Hall. Low-cost balloon missions to mars and venus. In *European Rocket and Balloon Programmes and Related Research*, volume 530, pages 285–291, 2003.
- [5] VV Kerzhanovich, JA Cutts, HW Cooper, JL Hall, BA McDonald, MT Pauken, CV White, AH Yavrouian, A Castano, HM Cathey Jr, et al. Breakthrough in mars balloon technology. *Advances in Space Research*, 33(10):1836–1841, 2004.
- [6] Kanika Garg and Thomas Kuhn. Balloon design for mars, venus, and titan atmospheres. *Applied Sciences*, 10(9):3204, 2020.
- [7] Andre Girerd and Andre Girerd. A case for a robotic martian airship. In 12th Lighter-Than-Air Systems Technology Conference, page 1460, 1997.
- [8] Wikipedia. NASA Mini-Sniffer, August 3 2022. Accessed on: 2022-08-03.
- [9] Anthony Colozza. Preliminary design of a long-endurance mars aircraft. In *26th Joint Propulsion Conference*, page 2000, 1990.
- [10] Stephen Smith, Andrew Hahn, Wayne Johnson, David Kinney, Julie Pollitt, and James Reuther. The design of the canyon flyer, an airplane for mars exploration. In *38th Aerospace Sciences Meeting and Exhibit*, page 514, 2000.
- [11] Mark Guynn, Mark Croom, Stephen Smith, Robert Parks, and Paul Gelhausen. Evolution of a mars airplane concept for the ares mars scout mission. In *2nd AIAA" Unmanned Unlimited" Conf. and Workshop & Exhibit*, page 6578, 2003.

- [12] Justin Kearns, Michiko Usui, Suzanne Smith, Steve Scarborough, Tim Smith, and David Cadogan. Development of uv-curable inflatable wings for low-density flight applications. In 45th AIAA/ASME/ASCE/AHS/ASC Structures, Structural Dynamics & Materials Conference, page 1503, 2004.
- [13] A Noth, Samir Bouabdallah, S Michaud, Roland Siegwart, and W Engel. Sky-sailor design of an autonomous solar powered martian airplane. In *Proceedings of the 8th ESA Workshop on Advanced Space Technologies for Robotics and Automation (ASTRA 2004) ESTEC, Noordwijk, The Netherlands, November 2-4, 2004*, pages F–03. European Space Research and Technology Centre (ESTEC), 2004.
- [14] Andrew Simpson, Arvind Santhanakrishnan, Jamey Jacob, Suzanne Smith, James Lumpp, David Cadogan, Matt Mackusick, and Steve Scarborough. Flying on air: Uav flight testing with inflatable wing technology. In AIAA 3rd" Unmanned Unlimited" Technical Conference, Workshop and Exhibit, page 6570, 2004.
- [15] Andrew D Simpson, Osamah A Rawashdeh, Suzanne W Smith, Jamey D Jacob, William T Smith, and JE Lumpp. Big blue: high-altitude uav demonstrator of mars airplane technology. In 2005 IEEE Aerospace Conference, pages 4461–4471. IEEE, 2005.
- [16] Andrew Simpson, Jamey Jacob, Suzanne Smith, Osamah Rawashdeh, James Lumpp, and William Smith. Big blue ii: Mars aircraft prototype with inflatable-rigidizable wings. In *43rd AIAA Aerospace Sciences Meeting and Exhibit*, page 813, 2005.
- [17] Michiko Usui, Jamey Jacob, Suzanne Smith, Stephen Scarborough, and David Cadogan. Second generation inflatable/rigidizable wings for low-density flight applications. In *46th AIAA/ASME/ASCE/AHS/ASC Structures*. Structural Dynamics and Materials Conference, page 1883, 2005.
- [18] Robert D Braun, Henry S Wright, Mark A Croom, Joel S Levine, and David A Spencer. Design of the ares mars airplane and mission architecture. *Journal of Spacecraft and Rockets*, 43(5):1026–1034, 2006.
- [19] Jamey Jacob, James Lumpp, Suzanne Smith, and William Smith. Multidisciplinary design experience of a high altitude inflatable wing uav for aerospace workforce development. In *44th AIAA Aerospace Sciences Meeting and Exhibit*, page 93, 2006.
- [20] Daniel Reasor, Ray LeBeau, Suzanne Smith, and Jamey Jacob. Flight testing and simulation of a mars aircraft design using inflatable wings. In 45th AIAA Aerospace Sciences Meeting and Exhibit, page 243, 2007.
- [21] Lisero Perez Lebbink. Uav mission design for the exploration of mars-esa/euroavia design workshop 2006. Georgia Institute of Technology, 2008.
- [22] Koji Fujita, Remi Luong, Hiroki Nagai, and Keisuke Asai. Conceptual design of mars airplane. Transactions of the Japan Society for Aeronautical and Space Sciences, Aerospace Technology Japan, 10(ists28):Te_5-Te_10, 2012.
- [23] Koji Fujita, Hiroki Nagai, and Keisuke Asai. Conceptual design of a miniature, propeller-driven airplane for mars. In 50th AIAA Aerospace Sciences Meeting including the New Horizons Forum and Aerospace Exposition, page 847, 2021.
- [24] C DeSouza. Conceptual design of an unmanned aerial vehicle for mars exploration (miscav). In Proceedings of the 44th Lunar and Planetary Science Conference, Bruxelles, Belgium, pages 1–2, 2013.
- [25] KR Ramsley and JW Head. Exploring mars with micro-uav squadrons and high data rate communications. In *46th Annual Lunar and Planetary Science Conference*, number 1832, page 1185, 2015.
- [26] Steven J D'Urso, Kyle Tsai, Parul Chadha, and Harry H Hilton. A systems engineering approach to the conceptual design of a martian uav. In 54th AIAA Aerospace Sciences Meeting, page 0214, 2016.
- [27] M Anyoji, M Okamoto, K Fujita, H Nagai, and A Oyama. Evaluation of aerodynamic performance of mars airplane in scientific balloon experiment. Fluid Mech. Res. Int, 1(3):1–7, 2017.
- [28] Mostafa Hassanalian, D Rice, and A Abdelkefi. Evolution of space drones for planetary exploration: A review. *Progress in Aerospace Sciences*, 97:61–105, 2018.
- [29] M Hassanalian, D Rice, S Johnstone, and A Abdelkefi. Performance analysis of fixed wing space drones in different solar system bodies. *Acta Astronautica*, 152:27–48, 2018.

- [30] Mostafa Hassanalian, Devyn Rice, Stephen Johnstone, and Abdessattar Abdelkefi. Planetary exploration by space drones: design and challenges. In 2018 Aviation Technology, Integration, and Operations Conference, page 3027, 2018.
- [31] Agnieszka Kwiek. Conceptual design of an aircraft for mars mission. *Aircraft Engineering and Aerospace Technology*, 91(6):886–892, 2019.
- [32] Julian Galvez Serna, Fernando Vanegas, Felipe Gonzalez, and David Flannery. A review of current approaches for uav autonomous mission planning for mars biosignatures detection. In *2020 IEEE Aerospace Conference*, pages 1–15. IEEE, 2020.
- [33] JK Rahul Jayawardana and T Sameera Bandaranayake. A review of unmanned planetary exploration on mars. Journal of the National Science Foundation of Sri Lanka, 46(3):201–216, 2018.
- [34] Ishan Mishra, Aayush Kumar, and Vanshaj Malhotra. Conceptual design of an unmanned aerial vehicle for mars exploration. *European Journal of Engineering and Technology Research*, 6(5):111–117, 2021.
- [35] Anthony J Colozza, Christopher J Miller, Brian D Reed, Lisa L Kohout, and Patricia L Loyselle. Overview of propulsion systems for a mars aircraft. Technical report, National Aeronautics and Space Administration, Glenn Research Center, 2001.
- [36] Kelly Corfeld, Roger Strawn, and Lyle Long. Computational analysis of a prototype martian rotorcraft experiment. In 20th AIAA Applied Aerodynamics Conference, page 2815, 2002.
- [37] LA Young, EW Aiken, V Gulick, R Mancinelli, and GA Briggs. Rotorcraft as mars scouts. In *Proceedings, IEEE Aerospace Conference*, volume 1, pages 1–378. IEEE, 2002.
- [38] Pierpaolo Pergola and Vittorio Cipolla. Mission architecture for mars exploration based on small satellites and planetary drones. *International Journal of Intelligent Unmanned Systems*, 4(3):142–162, 2016.
- [39] Witold JF Koning, Wayne Johnson, and Håvard F Grip. Improved mars helicopter aerodynamic rotor model for comprehensive analyses. *AIAA Journal*, 57(9):3969–3979, 2019.
- [40] Theodore Tzanetos, MiMi Aung, J. Balaram, Havard Fjrer Grip, Jaakko T. Karras, Timothy K. Canham, Gerik Kubiak, Joshua Anderson, Gene Merewether, Michael Starch, Mike Pauken, Stefano Cappucci, Matthew Chase, Matthew Golombek, Olivier Toupet, Marshall C. Smart, Stephen Dawson, Erick Blandon Ramirez, Johnny Lam, Ryan Stern, Nacer Chahat, Joshua Ravich, Robert Hogg, Benjamin Pipenberg, Matthew Keennon, and Kenneth H. Williford. Ingenuity mars helicopter: From technology demonstration to extraterrestrial scout. In 2022 IEEE Aerospace Conference (AERO), pages 01–19, 2022.
- [41] Anubhav Datta, Beatrice Roget, Daniel Griffiths, Gregory Pugliese, Jayanarayanan Sitaraman, Jinsong Bao, Lin Liu, and Olivier Gamard. Design of a martian autonomous rotary-wing vehicle. *Journal of aircraft*, 40(3):461–472, 2003.
- [42] Hanbing Song and Craig Underwood. A mars vtol aerobot-preliminary design, dynamics and control. In 2007 IEEE Aerospace Conference, pages 1–14. IEEE, 2007.
- [43] John Gundlach, IV. Unmanned solar-powered hybrid airships for mars exploration. In *37th Aerospace Sciences Meeting and Exhibit*, page 896, 1999.
- [44] Anthony Colozza, RC Michelson, et al. Planetary exploration using biomimetics. *NASA Institute for Advanced Concepts*, 2000.
- [45] Akira Oyama. Multiobjective design exploration of airplane for mars exploration. In 21st Workshop on Astrodynamics and Flight Mechanics, 2011.
- [46] Csaba Singer. Ultralight solar powered hybrid research drone. arXiv preprint arXiv:1304.5098, 2013.
- [47] Hervé Bézard, Thibault Désert, Thierry Jardin, and Jean-Marc Moschetta. Numerical and experimental aerodynamic investigation of a micro-uav for flying on mars. In *76th Annual Forum & Technology Display*, 2020.
- [48] Enrico Petritoli and Fabio Leccese. Unmanned autogyro for mars exploration: A preliminary study. *Drones*, 5(2):53, 2021.

SIZING OF SOLAR HYBRID UAV FOR MARS

- [49] Maxim Tyan, Nhu Van Nguyen, Sangho Kim, and Jae-Woo Lee. Comprehensive preliminary sizing/resizing method for a fixed wing-vtol electric uav. *Aerospace Science and Technology*, 71:30–41, 2017.
- [50] Josiah T VanderMey. A tilt rotor uav for long endurance operations in remote environments. PhD thesis, Massachusetts Institute of Technology, 2011.
- [51] Andre Noth. Design of solar powered airplanes for continous flight. PhD thesis, ETH Zurich, 2008.
- [52] Robin Shrestha, Moble Benedict, Vikram Hrishikeshavan, and Inderjit Chopra. Hover performance of a small-scale helicopter rotor for flying on mars. *Journal of Aircraft*, 53(4):1160–1167, 2016.
- [53] Koji Fujita, Hilal Karaca, and Hiroki Nagai. Parametric study of mars helicopter for pit crater exploration. In *AIAA Scitech 2020 Forum*, page 1734, 2020.